UNIVERSITY OF OKLAHOMA

GRADUATE COLLEGE

Multi-Material Extrusion-Based Additive Manufacturing: Refinement and Vertical Stacking in a Dual-Silicone DIW System

A THESIS

SUBMITTED TO THE GRADUATE FACULTY

In partial fulfillment of the requirements for the

Degree of

MASTER OF SCIENCE

By

SEAN JOHNSON

Norman, Oklahoma

2025

Multi-Material Extrusion-Based Additive Manufacturing:

Refinement and Vertical Stacking in a Dual-Silicone DIW System

A THESIS APPROVED FOR THE

SCHOOL OF AEROSPACE AND MECHANICAL ENGINEERING

BY THE COMMITTEE CONSISTING OF

Dr. Yingtao Liu, Chair

Dr. Hanping Ding

Dr. Wei Sun

Acknowledgements

I am eternally grateful to Dr. Liu, my advisor and committee chair, for his limitless personal care, support, and advocacy on my behalf throughout my master's degree, this thesis, and beyond. Your investment in my growth as a student and person made all this possible. Thank you to Connor Lawrence for lending your guidance in my continuation of your work.

To my committee members, Dr. Ding and Dr. Sun— your time and feedback are the difference between me graduating and not. Thank you for being willing to hop on board and push me to the finish line.

I would like to thank the Department of Mechanical Engineering at the University of Oklahoma for providing the resources, space, and flexibility to pursue this research, and the faculty and staff of Biomedical Engineering for giving me foundation as an engineer. Both played pivotal roles in shaping my technical foundation and opening the doors for this project to take shape.

To my supervisors, staff, and friends in Residence Life—thank you for being my home in Norman. Your support gave me stability, perspective, and lots of laughter and dear memories throughout this journey.

To my family and friends—thank you for always cheering me on, even from afar. Your encouragement, belief, and pride in me challenge me to reach new heights. You are my why. I love you all and hope to continue to make you proud.

Table of Contents

Table of Figures

Table of Tables

Abstract

This thesis advances previous research in multi-material extrusion-based additive manufacturing using Direct Ink Writing (DIW) to develop a more controlled, vertically capable printing process. Building on a dual-material pneumatic extrusion system created at the University of Oklahoma, this work focuses on refining material flow, optimizing print parameters, and exploring early-stage stacking behavior with silicone elastomers.

After replicating the original dual-material setup using EcoFlex 00-30 silicone with and without THI-VEX additive, print inconsistency and overspreading highlighted the need for systematic control. A nine-line matrix was developed to isolate the effects of pneumatic pressure and print speed. Results identified 5 psi and 200 mm/min as optimal for consistent, single-layer deposition.

Two-pass stacking trials then tested three THI-VEX concentrations (15%, 20%, and 25%) to assess Z-axis behavior. Dimensional analysis showed the 20% formulation provided the most stable stacking, balancing stiffness with print reliability.

Though time constraints and dimensional limitations prevented multilayer stacking, this work establishes a repeatable framework for future Z-axis development in dual-silicone DIW systems. The findings transition this project from exploratory replication to process refinement, providing a validated path forward for additive manufacturing of soft, multi-material structures.

Chapter 1: Introduction & Literature Review

1.1: Overview of Additive Manufacturing & Silicone Rubber Printing

Traditionally, manufacturing has depended on subtractive techniques—milling, turning, and casting—which remove material from a solid block to reach the final form. These methods are still essential tools used for high-precision components, but can be inefficient in complex geometries, often generating excessive material waste (Paul & Anand, 2015). Additive manufacturing (AM) offers an alternative with greater design flexibility and material efficiency by building structures layer by layer (Gibson et al., 2015). Since its early developments in the 1980s, AM has grown from simply rapid prototyping to an advanced manufacturing tool used across multiple industries, from aerospace to biomedical engineering (Hull, 1986).

A leading AM technique called Direct Ink Writing (DIW) has become popular for its ability to create soft, flexible, and biocompatible materials. Unlike other AM techniques such as Fused Deposition Modeling (FDM) or Stereolithography (SLA), which, respectively, involve melting thermoplastics or curing resins, DIW extrudes high viscosity inks through a nozzle with precise control. This makes DIW especially useful for applications in soft robotics, biomedical implants, and wearable electronics (Zhou et al., 2020). The challenge is the precise rheological control needed over the material's flow to keep it stable after its deposition while still needing post-processing, like thermal or UV curing (Stang et al., 2023).

One material that works well with DIW is silicone rubber, particularly EcoFlex 00-30, a platinum-catalyzed silicone that vulcanizes at room temperature. EcoFlex 00-

30 has impressive properties, including being able to stretch up to 900% and having a low hardness rating (Shore 00 scale hardness of 30), which makes it feel as soft as a gummy bear (Smooth-On, n.d.). These properties prime it for the aforementioned applications, more specifically, prosthetics, soft actuators, stretchable sensors, etc. (Kim et al., 2018). Printing with silicone is tricky due to its thickness and curing process. It requires careful control over how fast the material is extruded, how it spreads, and how the layers bond together to create stable and durable prints (Duty et al., 2018).

Connor Lawrence's research at the University of Oklahoma progressed DIW silicone printing by implementing a dual-material nozzle system and improving print quality through refining parameters of material composition, extrusion, and pressure control (Lawrence, 2024). His work was almost exclusive to geometries in the X-Y plane, leaving the viability of Z-axis stacking and structural integrity in multi-layer deposition largely untested. Lawrence's findings also contributed to improving flow consistency, but missed the key aspects of microstructural defects, void formation, and mechanical durability, which remain underexplored.

Building on this foundation, this thesis investigates how modifications in material formulation and process parameters affect Z-axis printability and structural integrity in multi-layered silicone rubber prints. By further testing extrusion pressure, and THI-VEX concentration with custom G-code strategies, this study aims to extend DIW capabilities beyond single-layer deposition. The next section will outline the specific challenges in multi-layer silicone rubber printing, and Section 1.3 will discuss how prior research has addressed similar issues and what gaps remain.

1.2: Challenges in Soft Material and Multi-Layer Printing

While DIW has become a promising technique for printing soft, flexible materials, consistent multi-layer stacking—especially using silicone rubber—remains a complex and underdeveloped area. The core of the challenge lies in the material's behavior prior to curing. Silicone rubber, particularly two-part Room Temperature Vulcanizing (RTV) formulations like EcoFlex 00-30, maintains a semi-liquid, viscous state after extrusion. Unlike thermoplastics used in FDM, which solidify rapidly upon cooling, silicone materials require a longer curing period, introducing risks of sagging, layer deformation, or uncontrolled spreading during and after deposition (Zhou et al., 2020).

The difficulty of stacking layers vertically stems from several interconnected factors. First is the rheological control required to ensure consistent extrusion. Pneumatic systems used in DIW must finely balance pressure with viscosity to prevent over- or under-extrusion. Even slight deviations in either pressure or flow consistency can produce uneven layer heights, excessive spreading, or gaps between extruded paths. Moreover, nozzle behavior plays a significant role in how cleanly the material is deposited; irregularities in tip geometry or misalignment can result in deposition that deviates from the intended path (Duty et al., 2018).

To address these limitations, researchers have experimented with thixotropic agents such as THI-VEX, which increase the material's viscosity and enhance its ability to hold shape after extrusion. These additives help reduce spreading by temporarily thickening the silicone under low shear conditions, allowing it to support itself between layers. However, striking the correct balance is nontrivial. Excessive thickening can make extrusion mechanically difficult, risking inconsistent flow or nozzle clogging, while insufficient viscosity leads to deformation and print failure (Abdollahi et al., 2018).

Another important consideration in multi-layer silicone printing is dimensional fidelity along the Z-axis. While many DIW studies focus on achieving high-resolution features in the X-Y plane, vertical stacking introduces new demands. Interlayer adhesion must occur reliably without the benefit of active cooling or photopolymerization to "lock in" previous layers. If the layer below is too soft, the new deposit may deform it. If it is partially cured, adhesion may be weak or incomplete. Researchers have not yet fully resolved the timing and mechanics of layering to ensure both structural integrity and functional bonding (Stang et al., 2023).

Furthermore, microstructural issues such as voids, air bubbles, surface defects, and uneven material density can accumulate with each additional layer. While this thesis does not focus on micro-level characterization, these defects are known to affect the mechanical and functional performance of soft components—especially in critical applications like biomedical implants or stretchable electronics (Kim et al., 2018). Understanding how layer-by-layer variability contributes to these effects is an important consideration for future DIW development.

In prior work at the University of Oklahoma, Lawrence developed a dual-material DIW system aimed at improving flow control and print consistency for single-layer silicone geometries. His work demonstrated that material mixing, pre-curing time, and pneumatic pressure adjustments could dramatically influence print quality. However, his experiments remained limited to planar deposition, and his system did not fully explore the effects of stacking, vertical resolution, or interlayer bonding dynamics. As a result, several challenges—including pressure ramping, sag mitigation, and layer interface stability—remain unresolved.

This thesis builds upon that foundational work, shifting focus from 2D fidelity to the more complex challenge of multi-layer deposition. In doing so, it addresses not only material flow and rheology but also the mechanical behavior of printed structures under gravitational and curing constraints. These challenges require both experimental rigor and strategic modifications to process parameters and toolpath control, which are explored in the chapters that follow.

1.3: Existing Research and Technical Gaps

Over the past two decades, DIW has evolved into a key technique for fabricating complex structures from soft materials, especially elastomers and biocompatible polymers. Unlike traditional extrusion-based techniques that rely on thermal phase transitions, DIW can operate at room temperature with materials like silicone rubber, hydrogels, and conductive pastes. This makes it uniquely suited for applications where flexibility, softness, or custom material formulations are critical (Duty et al., 2018). Despite this promise, a persistent limitation across the literature is the difficulty of achieving reliable, precise multi-layer prints—especially in vertically stacked geometries.

Much of the existing research has focused on extrusion parameter tuning, including pneumatic pressure regulation, nozzle geometry, print speed, and material pre-treatment. For instance, studies have shown that slight increases in pressure can compensate for more viscous formulations, but only up to a point—beyond that, over-extrusion causes dimensional inaccuracy and instability in layer formation (Abdollahi et al., 2018). Similarly, slow print speeds improve deposition accuracy but increase the risk of premature curing, which can compromise layer bonding.

A widely adopted strategy for enhancing print fidelity involves incorporating viscosity modifiers like THI-VEX, fumed silica, or other thixotropic agents. These additives increase the material's yield stress, allowing it to retain its shape after deposition while remaining extrudable. However, with pneumatic pressure, their benefits are contingent on fine-tuned concentration levels. Even minor deviations can make the mixture too stiff to extrude or too runny to maintain structure. Despite many experimental trials, there is no standardized formulation for multi-layer silicone printing—particularly when custom toolpaths or dual-material systems are involved.

Lawrence’s work is one of the more methodical efforts to optimize silicone DIW printing at the University of Oklahoma. His research introduced a dual-material extrusion system with pneumatic control and modified G-code, enabling material switching and improved flow consistency. By incorporating 15% THI-VEX and a 15-minute pre-curing period, Lawrence demonstrated that smoother extrusion and better shape retention were achievable in single-layer structures. His experiments also revealed how pressure fluctuations and nozzle switching influenced deposition quality. However, his scope was limited to planar (X-Y) geometries, and questions about Z-axis layer adhesion, repeatability, and structural stability were left largely unexplored (Lawrence, 2024).

Beyond Lawrence's contributions, other research groups have proposed hardware and software innovations to improve DIW’s vertical resolution. Some teams have explored adaptive pressure modulation, where pneumatic pressure is dynamically adjusted mid-print to compensate for material flow inconsistencies. Others have employed UV-assisted or thermal curing strategies to solidify each layer rapidly after deposition. These methods help reduce sagging but introduce complexity in timing and thermal management. Still, few studies have demonstrated robust, repeatable Z-axis stacking for silicone-based inks under ambient curing conditions (Stang et al., 2023).

Among the persistent gaps in the field, three stand out:

1. **Material Flow and Spreading in Multi-Layer Prints**

   Although THI-VEX and similar agents can improve shape retention, few studies have systematically analyzed their impact on multi-layer behavior, particularly with respect to curing time and interlayer adhesion. Excess spreading remains a key barrier to vertical fidelity (Zhou et al., 2020).

2. **Interlayer Bonding and Structural Integrity**

   Most existing work focuses on ensuring adhesion to the substrate or between adjacent lines, but not vertical interfaces. The curing window between layers is narrow, and mistiming can result in weak bonds or internal delamination (Kim et al., 2018).

3. **Customized G-code for Vertical Stacking**

   Most DIW processes use generic slicers and toolpaths not designed for pneumatic or non-Newtonian materials. Custom-written G-code offers an opportunity to synchronize movement, pressure, and extrusion timing more precisely, yet very few implementations exist in the literature.

This thesis directly addresses these gaps by combining material formulation trials, parameter optimization, and G-code engineering. Through systematic testing of THI-VEX concentrations and extrusion settings, alongside iterative refinement of print commands, this study provides a framework for more robust, scalable multi-layer printing using DIW and silicone rubber.

1.4: Research Objectives & Significance

The central objective of this study is to develop and validate a systematic approach for achieving consistent, high-fidelity multi-layer DIW printing with silicone rubber. While single-layer printing has been largely optimized in recent work, the ability to print vertically stacked, structurally sound silicone parts remains limited. This thesis extends prior research by integrating material composition control, pressure-speed calibration, and custom G-code strategies into a unified workflow.

The research is guided by the following core goals:

- **Replicate and validate** established DIW printing conditions to ensure experimental reliability and system understanding.
- **Evaluate and optimize** THI-VEX concentrations to enhance viscosity without compromising extrudability or layer adhesion.
- **Fine-tune extrusion parameters**, especially pneumatic pressure and print speed, to determine ideal operating conditions for vertical stacking.
- **Develop and test custom G-code scripts** to improve synchronization between nozzle movement, pressure control, and Z-axis positioning.

These efforts are significant not only because they tackle an underexplored challenge in DIW but also because they could enable broader application readiness in medical and engineering fields. Improved multi-layer DIW processes would support the fabrication of more complex 3D geometries, including embedded structures, soft joints, and gradient materials—features that are difficult or impossible to achieve with conventional FDM or SLA techniques.

In addition, the research contributes to a growing body of knowledge around open-source hardware integration, process reproducibility, and modular toolpath development for soft materials. The use of G-code as a modifiable interface allows for broader accessibility and adaptability across research labs and industries using custom or low-cost DIW systems.

1.5: Thesis Outline

This thesis is organized to reflect the iterative and exploratory nature of the research, beginning with a foundational replication phase and progressing through experimental optimization and vertical stacking analysis. Chapter 1 introduces the context of additive manufacturing with a focus on DIW, highlighting the specific challenges associated with multi-layer silicone rubber printing. It reviews prior research efforts, including those by Lawrence, and outlines the core research objectives and significance of this study. Chapter 2 documents the replication of Lawrence's two-material DIW setup, including detailed observations of material preparation, pneumatic pressure configuration, and extrusion behavior. This replication phase established the experimental baseline and provided critical insight into the behavior of THI-VEX-modified EcoFlex during extrusion.

Building on this foundation, Chapter 3 presents a series of single-layer print tests designed to isolate and optimize key parameters such as pneumatic pressure, print speed, and G-code synchronization. A nine-line matrix test was developed to evaluate how different combinations of speed and pressure impacted print fidelity, consistency, and material behavior. These findings informed the selection of optimal settings for subsequent Z-axis trials. Chapter 4 then shifts focus to vertical stacking, beginning with two-layer prints and systematically evaluating the effects of different THI-VEX concentrations on structural stability and print quality. This chapter includes both visual and quantitative assessments of stacking precision, edge definition, and interlayer adhesion, offering insights into the feasibility and limitations of multi-layer silicone printing using current materials and methods.

Finally, Chapter 5 concludes the thesis by summarizing the key findings, acknowledging experimental limitations, and proposing directions for future work. Potential areas for improvement include refining nozzle designs, automating pressure control, and exploring alternative curing strategies. Collectively, this structure presents a logical and progressive exploration of DIW capabilities for soft material manufacturing, with each chapter building on the last to provide a comprehensive understanding of the transition from planar to multi-layer printing.

Chapter 2: System Replication and Process Familiarization

2.1: Experimental Setup & Materials

Replicating Lawrence's two-material silicone printing process was a critical first step toward building a foundation for this study. This phase focused on re-establishing Lawrence's baseline conditions—material preparation, pneumatic control, and printer behavior—while identifying any process sensitivities or areas for refinement in the context of future multi-layer experiments.

Material Preparation and Handling

EcoFlex 00-30 was used as the base silicone material due to its favorable mechanical properties for soft material printing. To improve shape retention during deposition, the thixotropic agent THI-VEX was incorporated into the formulation at 15% by weight, and the mixture was allowed to pre-cure for 15 minutes prior to extrusion. This exact protocol—based on Lawrence's methodology—served as the baseline material preparation process throughout the study.

Figure 1: THI-VEX Parts A and B

Figure 2: Unmodified EcoFlex 00-30 with Blue Food Coloring in Syringe Prior to Loading

The mixing procedure involved equal parts of Part A and Part B (5g each) with 1.5g of THI-VEX, stirred thoroughly until uniform. After pre-curing, the material was loaded into two 10 mL syringes corresponding to the left and right channels of the printer's dual-extrusion system. Degassing was not performed, as the mixture's viscosity and short open time limited visible bubble formation, though the potential for microbubbles remained a minor consideration.

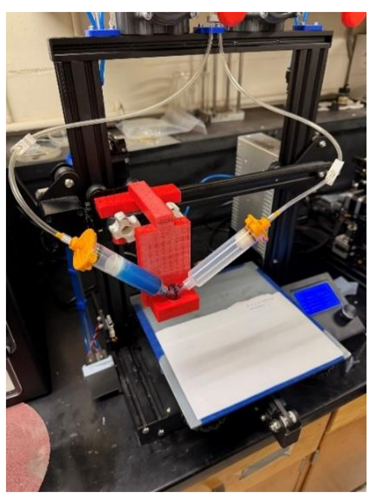

Figure 3: Unmodified Silicone Loaded into Extrusion System

Printer Setup and Control System

The printing system consisted of a modified Creality Ender 3 equipped with Lawrence's custom dual-material pneumatic extrusion head. Solenoid valves regulated compressed air to each syringe, enabling toggling between material channels mid-print. The extrusion system was governed by G-code commands adapted from thermoplastic extrusion conventions: M104 and M106 were re-purposed to control valve opening and closing.

Initial toolpaths were generated via PrusaSlicer and edited manually to ensure correct valve actuation and synchronized motion. Notably, nozzle height and lateral calibration were carefully tuned to match the deposition behavior of the higher-viscosity mixture, which responded differently than unmodified EcoFlex.

Preliminary Observations with Single-Material Prints

Before executing a full two-material print, a single-material test was conducted using blue-dyed EcoFlex (without THI-VEX or pre-curing) to establish a baseline. As expected, the unmodified silicone exhibited poor structural stability—lines spread immediately after deposition, producing undefined geometries with minimal adherence to the intended toolpath. These early tests reaffirmed prior findings and highlighted the importance of viscosity control.

When the THI-VEX-modified formulation was introduced under the same printing conditions, material behavior improved dramatically. The deposited lines retained their width more reliably, adhered consistently to the surface, and showed significantly less spreading. These results aligned with expectations based on

Lawrence's protocol and validated the formulation as a suitable starting point for further experiments.

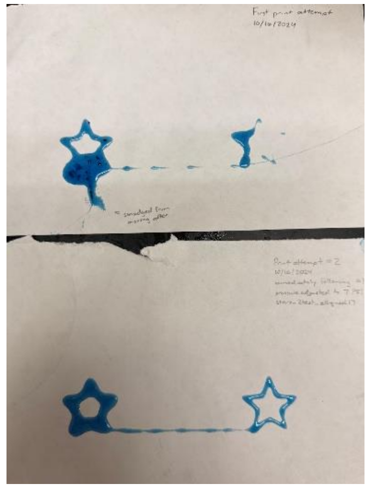

Figure 4: Early Print Attempts Without THI-VEX or Pre-Cure at 5 psi and 7 psi

Baseline Two-Material Print and System Evaluation

A full two-material print was then performed using Lawrence's original G-code with the 15% THI-VEX formulation. The selected parameters—5 psi pneumatic pressure and 200 mm/min print speed—served as the baseline operating point. During the print, both material channels activated as intended, and the extrusion system produced continuous lines with relatively consistent geometry across the pattern.

Minor issues such as brief start-up lag and slight thickness variation were observed, echoing prior reports. These were attributed to pressure ramp-up time and valve actuation delay—challenges that would be addressed in subsequent chapters.

Overall, the print validated the equipment configuration and provided confidence in the setup's ability to execute controlled, multi-variable experiments.

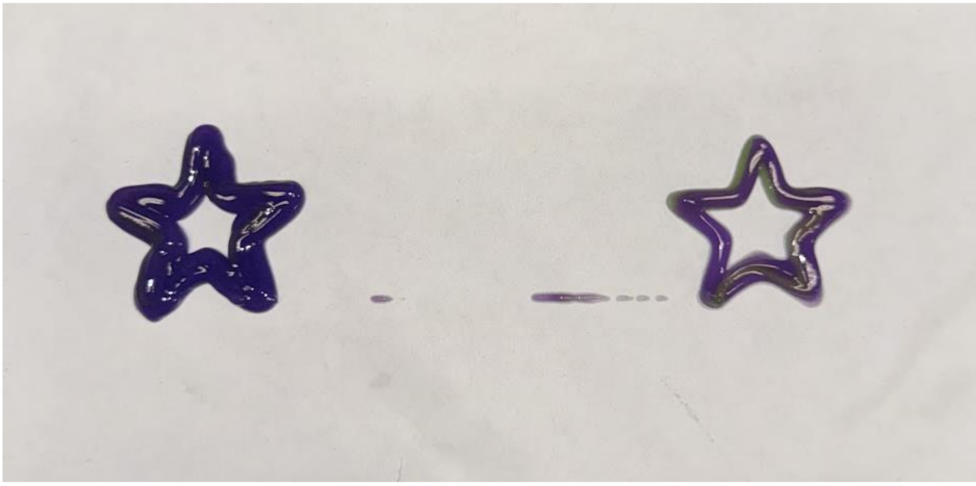

Figure 5: First Replication Attempt Using 15% THI-VEX and Pre-Cured Material

Takeaways and Foundation for Future Testing

This replication phase confirmed the necessity of viscosity tuning, demonstrated that Lawrence's setup could be reproduced reliably, and exposed subtle system dynamics—such as response lag and print-to-print variability—that would become important in more complex tests. With the experimental foundation in place, Chapter 3 focuses on a systematic investigation of print parameters—specifically pressure, speed, and line patterning—to identify conditions conducive to consistent deposition and ultimately, vertical stacking.

2.2: Reproducing the Dual-Material Process

The first full two-material print using Lawrence's baseline G-code marked the transition from system replication to process evaluation. This stage aimed to observe how the pneumatic DIW setup behaved under real conditions—highlighting system responsiveness, material flow dynamics, and practical deviations from expected print paths. Baseline parameters were maintained: 5 psi pneumatic pressure, 200 mm/min print speed, and a 15% THI-VEX-modified EcoFlex mixture with a 15-minute pre-cure.

Figure 6: Side-by-side curing of the two silicone formulations used in dual-material printing: EcoFlex 00-30 and THI-VEX additive with green food coloring (left) and with purple food coloring (right)

Real-Time Behavior and System Responsiveness

At the start of the print, a brief extrusion delay was observed. Although the solenoid valves were triggered correctly via G-code, material flow took approximately 5–10 mm of travel to stabilize. This lag left initial segments under-extruded or completely blank, suggesting that the pneumatic system required a short pressurization delay before steady-state flow was reached. This effect, previously noted in Lawrence's reports, reinforced the need for a pre-extrusion priming step—either as a static pressure dwell or a brief "dummy path" to purge and stabilize flow.

Once extrusion began consistently, the THI-VEX-modified silicone maintained its shape and followed the toolpath with good fidelity. However, minor thickness variation occurred across different lines, despite constant system settings. These irregularities pointed to subtle influences from residual pressure lag, differences in valve timing, or slight inconsistencies in material loading.

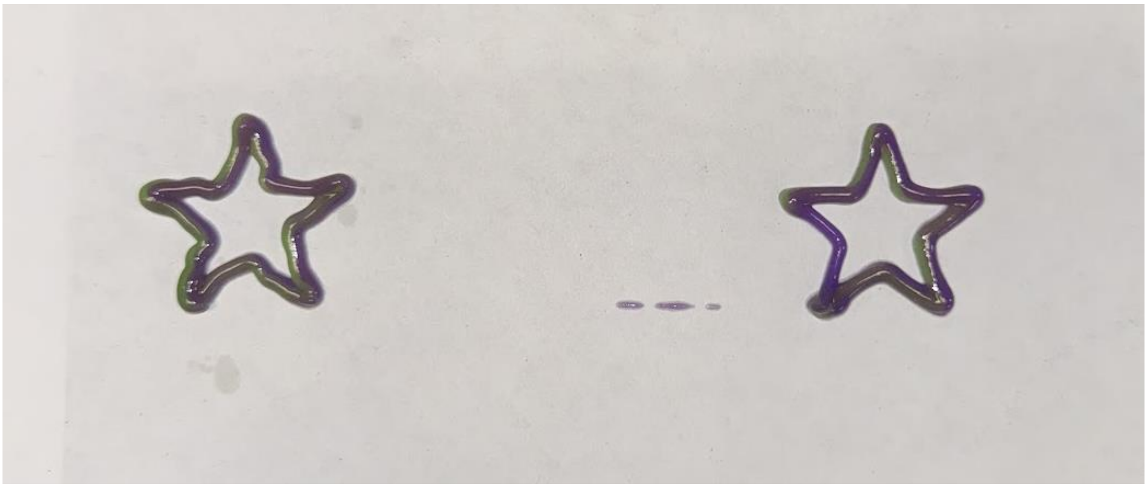

Figure 7: Second Replication Attempt at Identical Conditions

Speed–Pressure Interactions and Flow Sensitivity

Although this experiment used a single speed-pressure pair, brief adjustments revealed the system's high sensitivity to small pressure changes. Increasing pressure slightly above 5 psi immediately resulted in noticeable line thickening and material spreading, while lowering it below 5 psi produced under-extrusion and inconsistent paths. These effects were consistent with earlier replication results and confirmed that the operational window for consistent printing is narrow.

This behavior had critical implications for scaling: even minor variations in regulator output, air temperature, or material viscosity could cause performance drift. It also reinforced the need for tightly calibrated parameter sweeps, which would be explored systematically in Chapter 3.

Surface Interaction and Path Geometry

On the print surface, the silicone generally adhered well, though minor spreading and bulging occurred at line terminations or abrupt direction changes. These effects were most pronounced when extrusion continued for a split second after valve closure—what became known as the "tailing" artifact. As lines approached their endpoints, residual pressure caused a small blob or taper, especially when the nozzle stopped abruptly.

Gaps between adjacent lines were also noted, typically due to insufficient lateral overlap. While the G-code had been designed to create uniform spacing, slight misalignments in nozzle height or surface calibration likely contributed to inconsistent bonding. These defects weren't structurally catastrophic in this phase but foreshadowed challenges that could arise during vertical stacking, where layer continuity is essential.

Valve Timing and G-Code Responsiveness

While Lawrence's repurposed G-code commands (M104, M106) functioned effectively for basic valve control, the timing mismatch between nozzle movement and material flow remained a recurring issue. The lag at both the start and end of each print segment indicated that pressure actuation and valve response were not perfectly synchronized with tool movement.

This confirmed a need for future G-code refinement—specifically, the insertion of small dwell commands, pressure ramping strategies, or delayed shutoff sequences. Without these enhancements, flow dynamics at the segment boundaries would remain uncontrolled, compromising fidelity in more complex geometries or layered structures.

Summary and Transition to Parametric Testing

The initial full print trial established a functioning baseline but also exposed several key variables that demanded closer attention. Extrusion lag, tailing artifacts, pressure sensitivity, and inter-line spacing inconsistencies pointed to deeper system dynamics that couldn't be resolved through fixed settings alone. These findings provided the motivation for the controlled nine-line parameter test introduced in Chapter 3, designed to map the performance boundaries of the DIW process and identify optimal combinations of speed, pressure, and flow control.

2.3: Observations and Lessons from Replication

The replication phase served as both a technical validation of Lawrence's DIW setup and a critical learning experience in understanding the nuanced behavior of pneumatic silicone printing. While the print outcomes largely aligned with expectations, the process also revealed hidden variables and system sensitivities that would guide the structure of future experiments. By observing how material properties, extrusion mechanics, and G-code behavior interacted under controlled conditions, this phase clarified which elements were stable, which were problematic, and which held the potential for further refinement.

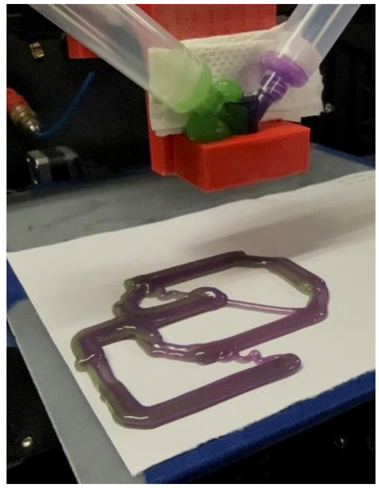

Figure 8: Supplemental OU Logo Print Using Remaining Materials

The Value of Replication as a Calibration Tool

Successfully replicating the two-material DIW print under Lawrence's parameters provided assurance that the modified Ender 3 system was functioning as intended. The consistency of deposition when using a 15% THI-VEX mixture, 5 psi pressure, and a 200 mm/min print speed demonstrated that the pneumatic setup could reliably execute multi-path prints with adequate fidelity. However, this phase also served a deeper purpose: it calibrated expectations for how small variations—whether in pressure, material preparation, or nozzle movement—could influence outcomes in non-obvious ways.

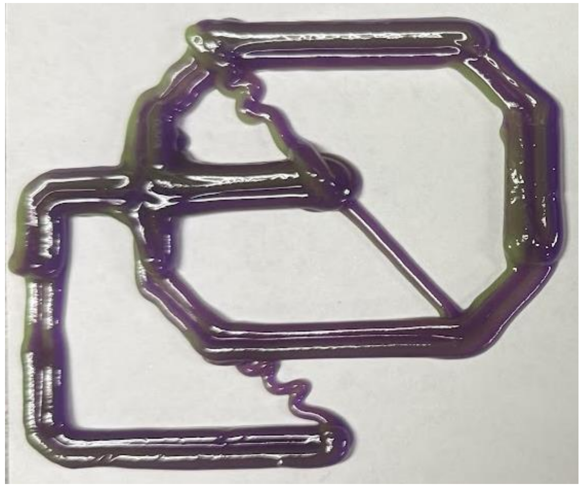

Figure 9: First Replication of OU Logo Demonstrating Extrusion Stability

For instance, although the print appeared clean overall, close inspection revealed micro-level inconsistencies in line thickness, edge sharpness, and start/end control. These variations were not random; rather, they reflected the interplay of hardware limits and material response time. Replication thus transitioned from a mechanical exercise to an observational diagnostic tool, offering a lens into the dynamic behavior of the printing system.

System Sensitivities: Pressure, Flow, and Feedback Delay

While it was anticipated that pneumatic pressure would influence flow rate, the extent of this sensitivity became more apparent during replication. Even minor adjustments around the 5 psi mark produced immediate and visible changes in deposition behavior. At 6 psi, lines became noticeably thicker, with rounded edges and greater spreading. At 4 psi, the system produced intermittent gaps, especially in corners and narrow features. These results highlighted the non-linear behavior of material flow relative to pressure—a key insight that would later shape the design of the parameter sweep in Chapter 3.

Equally important was the observation that response delays existed at both the hardware and material levels. The extrusion lag at the start of a print pass and the residual “tailing” at its end were not just valve issues—they were system-level timing mismatches resulting from compressed air dynamics, nozzle backpressure, and silicone rheology. These insights suggested that without tighter control of start/stop timing, increasing the complexity or verticality of prints would compound inaccuracies.

G-Code Interpretation and Valve Behavior

The repurposing of thermoplastic printer commands (M104, M106) for pneumatic valve actuation was effective but not without limitations. The valves operated on a binary open/close logic, which lacked the finesse to handle nuanced pressure transitions. Additionally, the printer’s firmware interpreted these commands without regard for the physical delays involved in air pressurization or depressurization.

This disconnect became apparent during material switching and segment transitions. Although the toolpath commanded a clean movement, the material deposition lagged behind by fractions of a second—enough to leave gaps, bulges, or unwanted artifacts. These findings highlighted the importance of future G-code customization, not just for path planning but for dynamically managing timing. Considerations for pre-extrusion delays, staggered shutdowns, and synchronized movement-pressure coordination emerged as central needs for progressing toward multi-layer prints.

Material Handling Variability and Consistency Risks

Despite careful attention to mixing, syringe loading, and pre-curing, minor differences in material consistency were observed across different batches. This variability—likely influenced by room temperature, mixing speed, or operator technique—manifested in slightly different extrusion behaviors even when parameters were held constant. While these differences did not derail the print, they raised concerns about repeatability in longer or more complex prints. The tactile nature of DIW, particularly with RTV silicones, leaves little room for procedural error—making process standardization a top priority for future testing phases.

A related observation involved syringe fill levels and extrusion behavior. As the volume of material decreased during printing, changes in backpressure were observed. This dynamic likely resulted from reduced internal resistance in the syringe barrel or air cushion behavior. While not formally measured in this phase, this variability would be important to track during extended print jobs or multi-layer stacking attempts, where consistent line quality across height becomes crucial.

Practical Implications for Vertical Stacking

Although no stacking was attempted in this chapter, several implications for future vertical printing became clear. First, the tailing effect at the end of lines would likely cause material bulges at layer transitions if left unaddressed. Second, pressure inconsistencies would amplify layer misalignments over time, particularly if the system failed to reach equilibrium between layers. Third, the curing interval between layers—currently left uncontrolled—would play a major role in how each new layer bonds to the one below it. Print timing, nozzle temperature, and even ambient humidity might become relevant variables as the Z-dimension is introduced.

More broadly, these observations confirmed that vertical DIW printing cannot rely on planar print heuristics alone. Whereas single-layer printing tolerates minor fluctuations without noticeable defects, multi-layer structures magnify these imperfections with each additional pass. Addressing these compounding effects would require a move toward closed-loop control, refined motion planning, and potentially new material formulations or nozzle strategies.

Summary and Research Direction

The lessons from this phase established a clear technical baseline while illuminating the system's inherent sensitivity. Conclusions included:

- Replication was successful and reliable, but not robust across variable conditions.
- Small pressure changes yielded large effects on print fidelity.
- Timing mismatches between G-code commands and material flow caused repeatable, observable artifacts.
- Material batch variation introduced subtle but important inconsistencies, emphasizing the need for standardized preparation.
- Without G-code refinement, current valve controls lacked the precision necessary for stacking.

These findings informed the design of Chapter 3's parameter sweep, which was developed to methodically test combinations of speed, pressure, and material properties across a fixed print pattern. The goal was to shift from qualitative observation to quantitative evaluation, enabling a data-driven approach to refining the DIW process for future multi-layer applications.

Chapter 3: Single-Layer Testing & Parameter Optimization

3.1: Rationale and Design of the Nine-Line Matrix

While the two-material replication in Chapter 2 confirmed that silicone printing via DIW could be achieved with reasonable consistency, it also revealed the limits of the approach used in prior work. Lawrence's methodology successfully demonstrated how thixotropic additives and pneumatic control could be used to print flexible silicone features, but his experimental process was primarily exploratory—relying on trial and error with broad adjustments in speed and pressure. This approach yielded meaningful insights but lacked the precision necessary to truly characterize the behavior of the system.

The replication process emphasized just how sensitive the system was to even minor changes in extrusion pressure or print speed. At Lawrence's recommended 5 psi and 200 mm/min, prints were clean and well-defined. But slight increases in pressure caused visible spreading and deformation. Similarly, changes in print speed affected the timing and consistency of material flow, introducing under-extrusion or trailing artifacts. These findings suggested that DIW with silicone was operating within a much narrower window of stability than previously understood. Small variations in parameters could push the system from optimal behavior into complete failure.

This sensitivity had important implications. If the goal was to build multi-layer, vertically stacked structures, then the material could no longer just "work most of the time." It had to behave reliably and predictably across prints. This would require a deeper understanding of how small parameter shifts affected material flow, line formation, and structural stability. Without that knowledge, stacking tests would be built on a shaky foundation, introducing variability that could not be easily diagnosed or controlled.

To address this, a refined testing methodology was developed. Rather than adjusting one variable at a time and observing qualitative outcomes, a controlled matrix of test conditions was constructed to evaluate combinations of pressure and speed systematically. The idea was to bracket the working values found during replication—specifically 5 psi and 200 mm/min—with a narrower range of settings. This allowed for targeted evaluation without introducing the confounding variability of larger jumps or untested extremes.

Additionally, this approach enabled identification not just of “what works,” but of how each variable interacts with the other. For example, increasing pressure may be tolerable at higher speeds but not at lower ones. Similarly, a slower speed might improve deposition at lower pressures, but introduce trailing at higher ones. These kinds of interactions are difficult to isolate through informal testing, but they become easier to spot when visual results are laid out in a clean, side-by-side matrix.

This motivation underpinned the design of the nine-line test, which formed the experimental core of Chapter 3. By testing all combinations of three pressure levels (5, 7.5, and 10 psi) and three speeds (150, 175, and 200 mm/min), a total of nine print conditions could be analyzed within a single, consistent framework. Each line in the pattern represented one parameter pair, allowing for rapid visual comparison and reliable annotation. As the following sections will show, this method clarified both the limitations of the DIW system and the specific combination of parameters most suitable for future vertical stacking.

3.2: G-Code Development and Process Control

With the need for a more refined understanding of extrusion behavior established, the next step was to design a controlled experiment capable of evaluating speed and pressure combinations systematically. The test had to isolate key variables, minimize external sources of variability, and produce results that could be directly compared within a single print session.

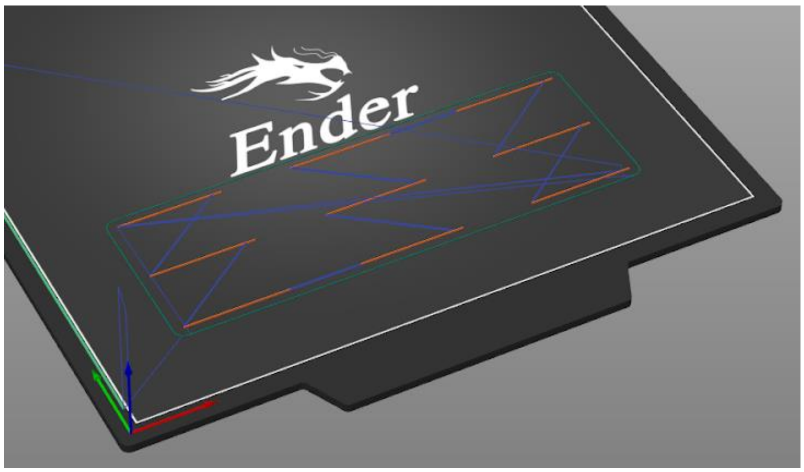

Figure 10: Sliced 3D Model of Nine-Line Test Geometry

A 3×3 test matrix was selected as the core framework. This approach allowed for nine unique combinations of three print speeds—150 mm/min, 175 mm/min, and 200 mm/min—and three pneumatic pressures—5 psi, 7.5 psi, and 10 psi. These values were chosen to bracket the known working settings identified during replication in Chapter 2 (5 psi and 200 mm/min), while also providing a finer resolution than the broader, exploration ranges used in previous research. The intention was not to re-discover what worked, but to pinpoint where material control began to degrade and to characterize how sharply performance dropped outside the ideal range.

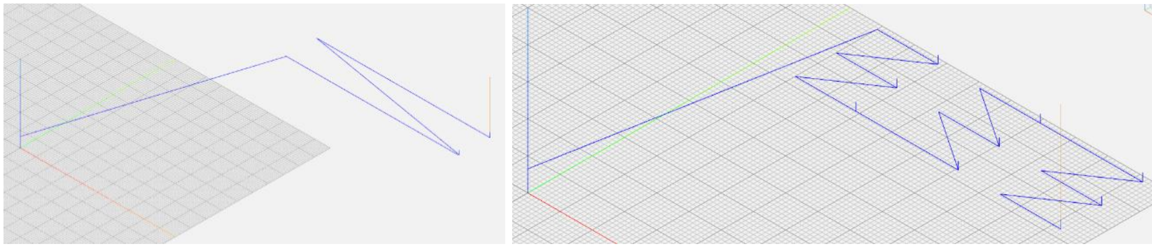

Figure 11: Comparison of Lawrence's Test v Final Nine-Line Output

Each line in the pattern represented a single speed/pressure pairing, printed consecutively in a fixed order. The test layout was simple: nine straight lines, evenly spaced in the Y-direction, with all lines printed from left to right along the X-axis. This arrangement allowed for quick visual comparisons. The lines were separated by a fixed vertical spacing to eliminate merging or cross-contamination, and each one was annotated immediately after printing with its parameter code (e.g., S1P1 for 150 mm/min at 5 psi).

Material preparation remained constant throughout the test. Each print used the revised 15% THI-VEX formulation (1.75g additive to 10g total EcoFlex) with a 15-minute pre-cure. Syringes were loaded and mounted using the same method described in Chapter 2, and care was taken to ensure consistent nozzle height and bed leveling across all trials. These controls ensured that any observed differences in line quality could be attributed to the selected parameters—not to inconsistencies in material handling or printer setup.

To execute the pattern reliably, hand modifications were applied to the G-code exported from the slicer software. Each line used a G1 command for linear movement, an M106 command to open the valve, and an M107 to close it. Print speed was encoded in the F parameter of the movement command (e.g., F150 for 150 mm/min). A short delay (G4) was inserted after the valve-on command to allow air pressure to stabilize before motion began. This mitigated the common issue of under-extrusion at the start of a line caused by system lag.

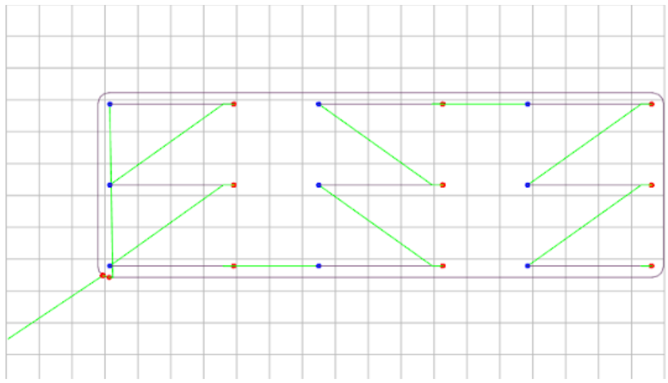

Figure 12: Initial Toolpath Preview for Nine-Line G-Code

Additional timing refinements were introduced after early tests showed excess material at the end of some lines. This “tailing” effect was addressed by adding a brief dwell between the valve-off command and nozzle lift. Through trial and error, a 300 ms delay at both the start and end of each line proved effective at balancing flow initiation and shutdown.

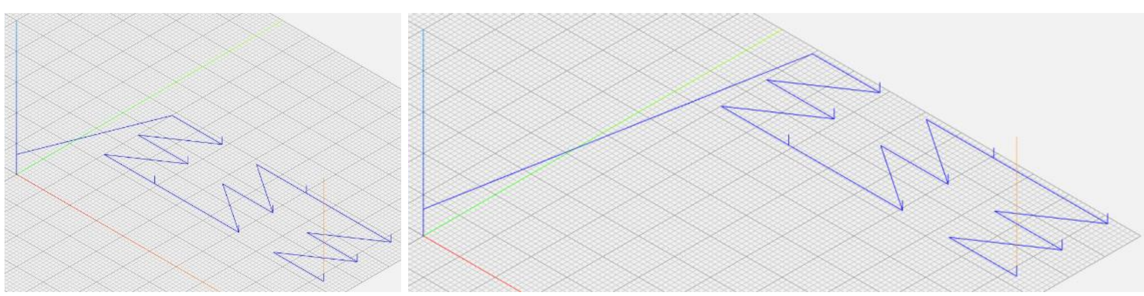

Figure 13: Toolpath Offset Correction to Maintain Bed Alignment

Each full matrix was printed using a single G-code file, with parameter combinations mapped to line order and annotated on the bed immediately after printing. This process was repeated multiple times to confirm consistency. Files were named and archived according to their parameter grid for future reference and comparison with stacking trials.

Table 1: Evolution of Nine-Line Toolpath Planning

	5 psi	7.5 psi	10 psi
150 mm/min	1→	2→	3↙
175 mm/min	4→	5→	6↙
200 mm/min	7→	8→	9

Table 2: Evolution of Nine-Line Toolpath Planning (Final Version)

	5 psi	7.5 psi	10 psi
150 mm/min	1↓	6→	7↓
175 mm/min	2↓	5↑	8↓
200 mm/min	3→	4↑	9

By combining a structured layout with controlled variables and refined execution, the nine-line matrix served as a critical stepping stone in the transition from replication to advanced parameter tuning. This confirmed the narrowness of the DIW working range, while laying the groundwork for identifying the specific conditions under which vertical stacking might be feasible. These conditions could be defended not by anecdotal success, but by repeatable, controlled testing.

3.3: Trial Results & Pattern Observations

The results of the nine-line test revealed a sharp contrast between stable and unstable extrusion conditions, underscoring the sensitivity of the DIW system to even modest changes in pneumatic pressure or print speed. By visually comparing all nine lines produced in a single print run, it became evident that only one setting—5 psi at 200 mm/min—produced consistent, high-quality results. The remaining combinations, including all trials at 7.5 and 10 psi, were visibly flawed, offering valuable insight into the boundaries of reliable material deposition.

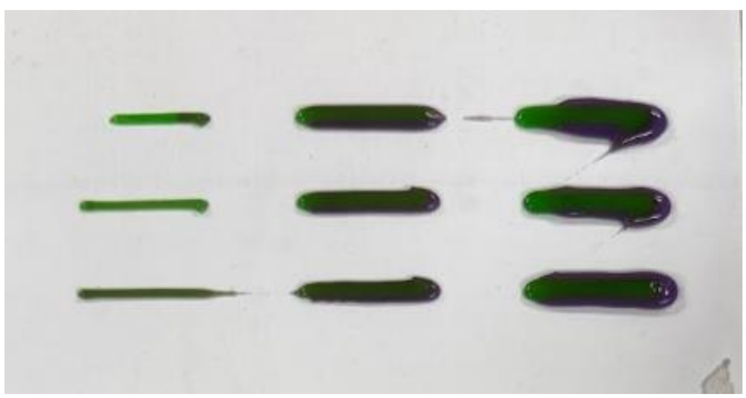

Figure 14: Trial 1 – Nine-Line Test

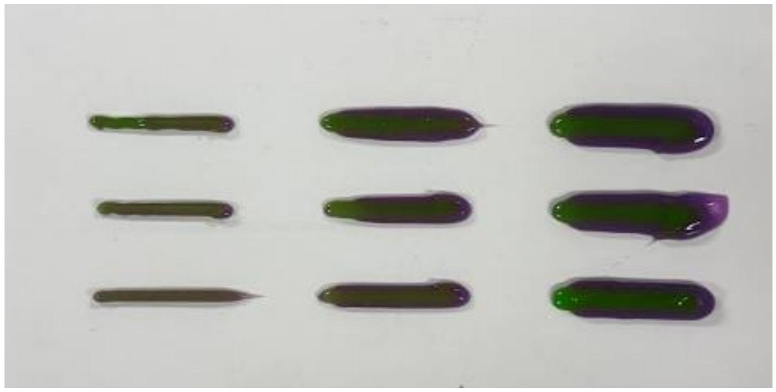

Figure 15: Trial 2 – Nine-Line Test

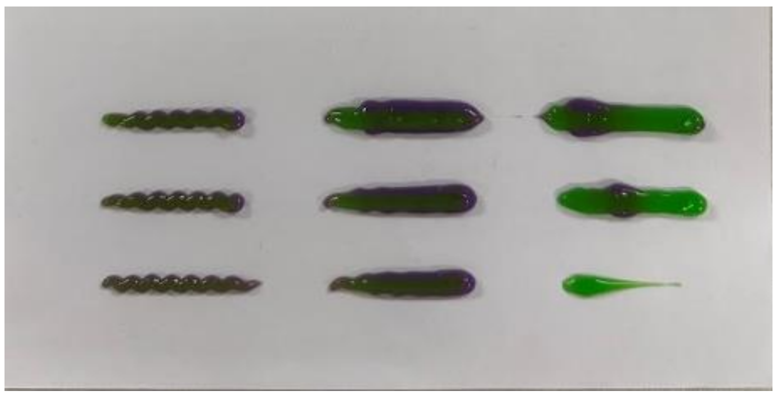

Figure 16: Trial 3 – Nine-Line Test

Across the matrix, three major failure modes were observed: over-extrusion, under-extrusion, and inconsistent flow behavior (such as tailing or wavering width). Each was strongly tied to pressure and speed settings, and each had implications for downstream print applications, particularly vertical stacking.

High Pressure: 7.5 psi and 10 psi

The most visually obvious failure mode appeared in the high-pressure prints. Lines printed at 10 psi—regardless of speed—consistently exhibited severe over-extrusion. At the lowest speed (150 mm/min), the nozzle moved slowly enough that material visibly pooled along the toolpath, resulting in bulbous lines with ragged edges.

The lines were not just oversized but visibly unstable, often displaying localized deformations at the start and end due to uncontrolled flow after valve shutoff.

Increasing the print speed slightly to 175 mm/min did not correct these issues. Although the nozzle moved more quickly, the system still pushed out too much material too fast. At 200 mm/min, the highest speed tested, over-extrusion was still apparent. In some cases, the speed was high enough to “drag” the excess material along the toolpath, but this created stringing and uneven trailing rather than proper deposition. At no point did 10 psi produce a line that could be considered suitable for stacking or further structural printing.

Prints at 7.5 psi were slightly better but still unsatisfactory. They exhibited many of the same issues seen at 10 psi—primarily over-deposition and trailing at the ends of lines—but to a slightly lesser degree. At 150 mm/min, excess material was still a problem, though the deformation was less extreme. At 175 mm/min, some lines appeared cleaner, but irregularities were still present. At 200 mm/min, 7.5 psi lines were narrower than those at lower speeds, but the material continued to overshoot the line ends after valve closure. In all three cases, edge definition was poor, and tapering or bulging made it clear these prints could not support vertical layers.

Low Pressure: 5 psi

The set of prints at 5 psi told a different story. At 150 mm/min, the extrusion was uneven and inconsistent. The system occasionally failed to deposit at all in one or both channels, resulting in broken or incomplete lines. This was likely due to insufficient air pressure to overcome backpressure in the syringe and nozzle, especially at a slower travel speed. While not as visibly messy as the high-pressure prints, these lines lacked reliability and would not support any structured layering.

At 175 mm/min, performance improved. Both channels deposited material more consistently, and the lines maintained better dimensional fidelity. However, some wavering in width was still observed along the length of the path, and trailing effects at line ends were not fully eliminated. These prints were close to usable but would still introduce variability in multi-pass or multi-layer prints.

The best result came from the 5 psi / 200 mm/min pairing. This combination produced even, well-defined lines with minimal trailing, no visible under-extrusion, and excellent consistency between the two print heads. The start and end points were clean, with no pooling or tailing, and the width remained constant across the full line. No other parameter combination in the matrix approached this level of control or repeatability.

Comparative Observations

One of the most telling observations from the matrix was that print quality did not vary linearly across speed or pressure. Increasing speed did not consistently offset the effects of higher pressure, nor did slowing down improve consistency at low pressure. Instead, each parameter interacted with the material's behavior and the system's responsiveness in a nonlinear way. The narrow window of successful operation—anchored entirely around 5 psi and 200 mm/min—suggests that the DIW system behaves more like a threshold-limited system than one that can be "tuned" freely across a broad operating space.

Another notable insight was how clearly the visual quality of each line reflected the underlying system dynamics. Inadequate pressure led to flow initiation problems, which were visibly marked by incomplete starts and thinning. Excess pressure overwhelmed the material's ability to hold shape, producing ballooning and stringing. Only at the correct pairing did the pressure build-up, nozzle movement, and valve actuation synchronize tightly enough to produce clean deposition.

These results validated the decision to test a narrow band of parameters rather than a wide one. Even within a constrained range, only a single condition proved reliably functional reinforcing the sensitivity of the DIW process and the importance of tightly controlled experimentation when working with soft, thixotropic materials.

In an effort to refine the quality of results across the nine-line matrix, I created and tested two additional iterations of the G-code. These versions modified non-variable aspects of the print process—such as valve timing, start delays, and toolpath offsets—while maintaining the validated settings of 5 psi and 200 mm/min. Since pressure and speed had already been established as the only viable operating conditions, these code revisions represented the last controllable elements available for optimization.

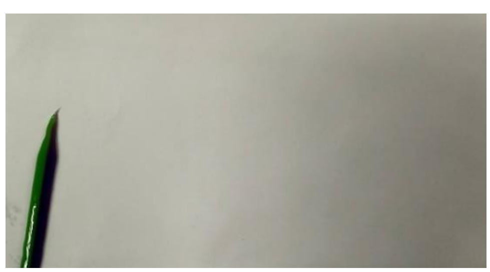

Figure 17: Exploratory G-Code Failure

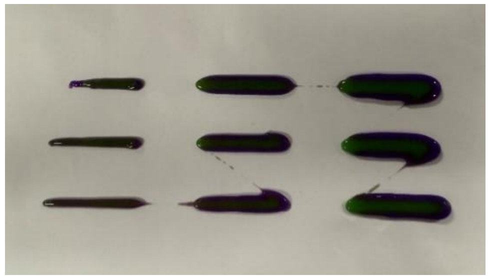

Figure 18: Exploratory G-Code Iteration – Unsuccessful Revisions

The resulting prints (Figures 20 and 21) did not yield any visual improvements. These trials reinforced the conclusion that the originally finalized G-code sequence—paired with the selected speed and pressure—was already operating at the upper limit of this setup's print quality. With the optimal condition established and no further gains available through G-code refinement alone, I was confident in moving forward, having fully explored the practical scope of this test matrix.

3.4: Selecting Parameters for Z-Axis Printing

The nine-line test confirmed that the DIW system, while capable of producing high-quality planar prints, operates within a narrow and unforgiving range of pressure and speed parameters. The fact that only a single parameter pairing—5 psi at 200 mm/min—consistently produced reliable prints was not a failure of the system, but a validation of its sensitivity. These results have direct implications for the transition to Z-axis printing, where each additional layer introduces compounding challenges.

The most immediate implication is that vertical stacking cannot tolerate the same level of variability tolerated in planar prints. In single-layer tests, over-extrusion might cause spreading or bulging, but the line still "works" in the sense that it adheres to the print surface. In vertical builds, those same inconsistencies distort the next layer or prevent it from bonding properly. This makes precision in material flow and deposition timing essential. The system must not only deposit the correct amount of material, but it must do so consistently across layers, with no irregularities at the start or end of each path.

This reinforces the importance of what was achieved in the nine-line testing phase: not simply finding a condition that works but understanding the bounds of the system's reliability. The clean result from the 5 psi & 200 mm/min pairing offered more than just aesthetic fidelity. It demonstrated that, under these settings, extrusion initiated and terminated cleanly, line width held steady throughout the path, and both material channels remained synchronized. This is precisely the type of behavior required for stacking—where each new layer must sit precisely atop the last with no sag, drift, or deformation.

Another key insight from the test matrix was that tuning pressure and speed independently is insufficient. Only when both are adjusted in concert can a usable operating point be found. Attempting to improve one by tweaking the other—such as increasing speed to mitigate excess pressure—produced only limited and unpredictable benefits. This means that, for vertical prints, parameter adjustments must be deliberate, coordinated, and minimal. A shift in pressure or speed in isolation could easily compromise layer alignment or bonding quality.

The nine-line test also emphasized the importance of extrusion timing, particularly valve actuation relative to nozzle movement. In planar printing, start-up lag or trailing may affect only the first and last millimeters of a line. But in stacked prints, these artifacts become structural flaws that alter the shape and surface of the print as it grows. The dwell adjustments and valve timing corrections tested during this phase were not just quality-of-life improvements; they were essential groundwork for enabling vertical consistency. Without them, line ends would pool or taper unpredictably, disrupting the Z-axis build-up.

Perhaps the most valuable implication of this test is methodology: it underscores the necessity of controlled, repeatable testing when transitioning from 2D to 3D prints in DIW. Prior work often relied on informal tuning, subjective visual inspection, or anecdotal success. The nine-line matrix demonstrated that even in a simple, controlled pattern, failure modes are easy to trigger and hard to diagnose without a systematic approach. It also showed that repeatability—across prints, across channels, and across sessions—is a prerequisite for any meaningful stacking test.

With a single, validated condition in hand, the study was finally positioned to move forward. The success of 5 psi and 200 mm/min wasn't just a coincidence—it was the product of controlled experimentation, guided by replication, narrowed by systematic testing, and confirmed by repeatable outcomes. It now serves as the baseline for all stacking attempts in Chapter 4, offering a platform from which to explore new variables—such as line spacing, layer curing time, and vertical deformation—in a controlled and defensible way.

The lessons from Chapter 3 are clear: DIW printing with silicone is a tightrope walk, not a wide runway. But with careful calibration and a systematic approach, it is possible to find and hold a balance--one line at a time, one layer at a time.

Chapter 4: Z-Axis Printing Results

4.1: Preparing for Two-Pass Z-Axis Testing

Motivation for Stacking in DIW

While the refinement of print parameters in Chapter 3 demonstrated that single-layer DIW silicone printing could be achieved with control and repeatability, it also raised the question of how far that reliability could be extended vertically. In any additive manufacturing process, the ability to build upward is what defines its structural utility. For DIW with soft materials like RTV silicone, the leap from planar prints to vertically stacked structures introduce a host of new challenges: interlayer bonding, deformation under gravity, material sag, and print timing all become critical.

The two-material prints in Chapter 2 and the parameter matrix in Chapter 3 were both fundamentally planar exercises. Even when lines were deposited next to each other in succession, each was laid on a flat surface, interacting only minimally with existing material. Moving into Z-axis testing—where a second layer is deposited directly on top of a previously printed line or shape—requires a shift in both process and mindset. Layer-on-layer stacking isn't just about repeating the same G-code at a higher Z-height; it's about understanding how one layer of silicone interacts with another under time-sensitive, pressure-driven conditions.

Given the material's thixotropic nature and cure-dependent structure, it wasn't clear whether a freshly deposited top layer would bond with the base layer or simply disturb it—causing spreading, bulging, or detachment. Likewise, it was unknown how much the base layer would support vertical growth without losing shape. Before any attempt at full 3D printing could be justified, it was necessary to first explore whether even a single stacked layer could be placed consistently, remain dimensionally stable, and form a clean interface with the layer below.

This chapter focuses on that question by exploring what will be referred to as "two-pass" Z-axis prints—cases where a second path is laid directly atop an existing line or shape, separated only by a short pause in printing and a controlled Z-height increase. These are not full multilayer prints in the traditional sense, but they represent the first deliberate step toward that goal.

Rather than building towers or complex geometries, the testing here focused on dual-layer line stacking using controlled geometry and validated print parameters (5 psi, 200 mm/min). The intent was to assess how different material formulations responded to this challenge, particularly how well the second layer adhered to the first without spreading or distorting it. If a stacked line grew wider than expected, it might suggest that the second pass was displacing material outward rather than bonding upward offering a measurable proxy for stacking quality.

To that end, three THI-VEX concentrations—15%, 20%, and 25% by weight—were tested using a consistent two-pass protocol. Visual inspection and manual width measurements were used to evaluate outcomes, with a specific focus on line definition, interlayer adhesion, and the overall shape integrity of the printed stack. While this work stops short of full multi-layer printing, it establishes a critical foundation: identifying the material and process conditions under which Z-axis growth becomes mechanically and geometrically viable.

Print Setup & Platform Changes

Executing reliable Z-axis prints requires a series of physical modifications to the printer setup to accommodate stacking and improve surface control. In earlier planar tests, prints were conducted directly on flat paper taped to the bed surface. While sufficient for one-layer deposition, this approach introduced too much variability for stacking attempts. The paper warped over time, absorbed ambient moisture, and introduced inconsistencies in material adhesion that became more problematic as the geometry grew vertically.

To address this, the print surface was switched to inverted plastic petri dish lids. These offered a flatter, more rigid base and better surface energy for silicone bonding. The transparency of the lids also aided in monitoring nozzle height and alignment during print setup. With a slight amount of pressure, the material adhered well to the plastic during the initial pass, and the smooth surface helped reduce drag or warping when the second pass was laid. Each lid was cleaned with isopropyl alcohol and affixed to the print bed using tape to prevent shifting.

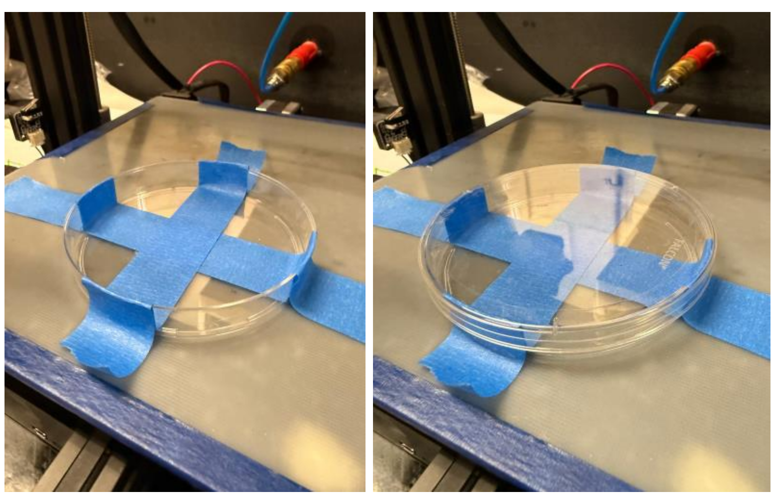

Figure 19: Print Setup with Replaceable Petri Dish Lid

At the outset of stacking trials, the last remaining pre-printed nozzles from Lawrence's original setup were used. To replace these aging nozzles, a new batch was printed using the Mono M5S SLA printer, with fresh resin. The goal was to replicate Lawrence's original design as closely as possible while improving print quality and material strength. However, some unexpected limitations arose. Removing the cured nozzles from the build plate proved more difficult than anticipated, occasionally damaging the nozzle tip or leaving unwanted excess.

Figure 20: SLA Printing of New Nozzles (1% and 100%)

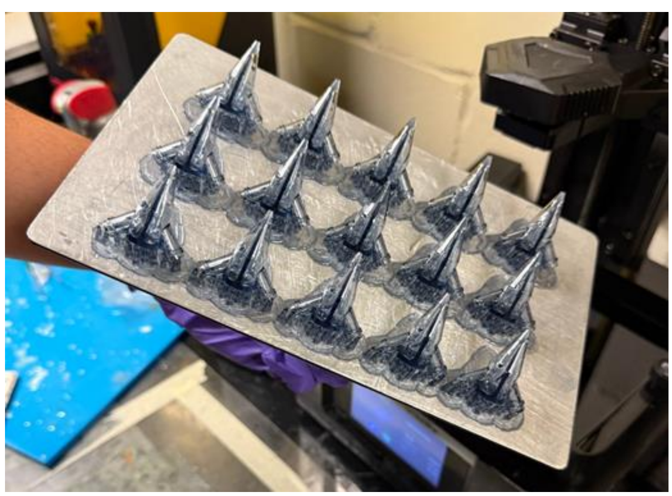

Figure 21: batch of 15 Resin printed Nozzles

Several of these printed nozzles were ultimately used in stacking trials, but not without workarounds. They were all scraped off the bed before being post-processed in a bath of isopropyl alcohol to remove uncured resin. Afterwards, tweezers were used to break and pull off extraneous and unwanted buildups that blocked critical junctures of the nozzles. While not ideal, these interventions allowed testing to proceed and helped underscore a recurring challenge in soft material DIW: tooling repeatability is as important as process control.

Figure 22: Tri-view of a Single-Printed Nozzle Removed from Build Plate

Figure 22: Nozzle Damaged in Post-Processing

Despite these hardware constraints, the basic two-pass tests were successfully run using Lawrence's nozzle design printed on the M5S. All trials were conducted with a validated Z-height offset between layers, and no further adjustments were made to pressure, speed, or G-code timing from the settings established in Chapter 3. By standardizing the mechanical and process setup, the study ensured that any variations in print quality or shape retention could be attributed primarily to material behavior—not equipment changes.

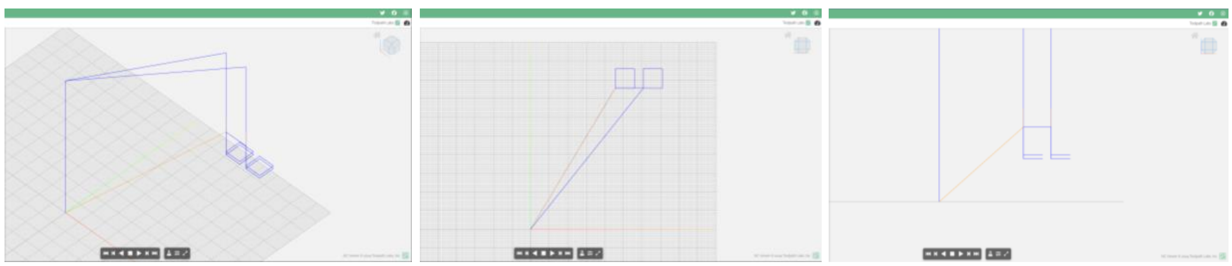

Figure 23: Visualized G-Code for Two-Pass Square Stack: Motion Path from Three Angles

Revised Mixing & Material Handling

While the base material used for these tests remained EcoFlex 00-30 mixed with THI-VEX additive, several procedural adjustments were necessary to accommodate the needs of the two-pass stacking trials. The most immediate change was in batch volume. In Chapter 3, replication and matrix tests used larger quantities of material, often exceeding what could be comfortably loaded into the 10cc syringes used for printing. For the stacking trials, each batch was deliberately scaled down to better match the syringe capacity and reduce waste. Smaller batches also helped preserve consistency during repeated trials, since older material tended to cure prematurely or behave inconsistently during extended testing sessions.

Three separate material formulations were prepared using THI-VEX at 15%, 20%, and 25% by weight of the combined Part A and Part B silicone. These ratios were selected to explore how increasing viscosity would influence the material's ability to support a second layer without deformation. The logic was simple: more THI-VEX should produce a stiffer, more shape-retaining material that resists being displaced when a second layer is deposited on top. However, it also came with risks—namely, that overly stiff formulations might not extrude cleanly or could resist bonding to the base layer.

Table 3: Material Formulations for THI-VEX Concentration Testing

	15% THIVEX	20% THIVEX	25% THIVEX
THIVEX	1.5 g	2 g	2.5 g
Ecoflex 00-30 A	4.25 g	4 g	3.75 g
Ecoflex 00-30 B	4.25 g	4 g	3.75 g
Total	10 g	10 g	10 g

Each batch was mixed by hand in small silicone-safe cups, using a lab scale to measure parts by weight. In chapters 2 and 3, a typical batch involved 5g Part A, 5g Part B, and the appropriate mass of THI-VEX to meet the target percentage: replication repeated Lawrence's 1.5g, the nine-line matrix utilized 1.75g. These formulations gave us 11.5-11.75 mL of material in tubes designed 10 mL capacity. With that in mind, the scaled down formulas were designed for all materials to add up to 10 g, excluding the drops of food coloring. 1.5g for 15%, 2g for 20%, and 2.5g for 25%. Once combined, the mixture was stirred thoroughly and pre-cured for 15 minutes before loading into syringes. This timing was based on prior trials and allowed the THI-VEX to thicken the silicone without advancing the cure too far, maintaining a balance between flow control and workability.

During handling, distinct differences between the formulations became apparent. The 15% THI-VEX batch remained relatively fluid and easy to mix but required more careful pressure control at the nozzle to avoid overspreading. By contrast, the 25% THI-VEX material was noticeably more viscous and required greater force to mix, unexpectedly posing the least resistance during printing and making flow less uniform between the two print channels. On occasion, air bubbles became trapped during syringe loading and were harder to purge from the thicker mixture, potentially introducing inconsistencies between trials.

The 20% THI-VEX formulation occupied the middle ground. It showed improved shape retention compared to the 15% batch while still extruding relatively smoothly through the nozzle without requiring excessive pressure. This formulation became the most promising candidate for continued testing, though all three were evaluated in parallel for comparison.

Across all conditions, attention was paid to how easily the material could be loaded, whether it resisted flow or backpressure in the syringe, and how well it adhered to the base layer during stacking. These characteristics, though not formally quantified—played an important role in determining print consistency and the interpretability of results in later sections. Material that spread too easily or flowed unevenly from trial to trial was less likely to produce a useful stacking geometry, even if it appeared dimensionally consistent in isolated prints.

With mixing protocols finalized and material batches prepared, testing moved forward into two-pass stacking trials using each THI-VEX concentration. These trials served as the core of Chapter 4, focusing on visual inspection, line shape preservation, and width measurements to evaluate stacking performance across material types

4.2: Two-Pass Print Results and Observations

Once all three THI-VEX formulations were prepared and loaded, two-pass stacking trials were performed using a consistent geometry across each test: a base square or line was printed, followed by a second pass directly on top at an increased Z-height. All tests used the previously validated baseline settings of 5 psi and 200 mm/min, and the only variable across trials was the THI-VEX concentration in the silicone.

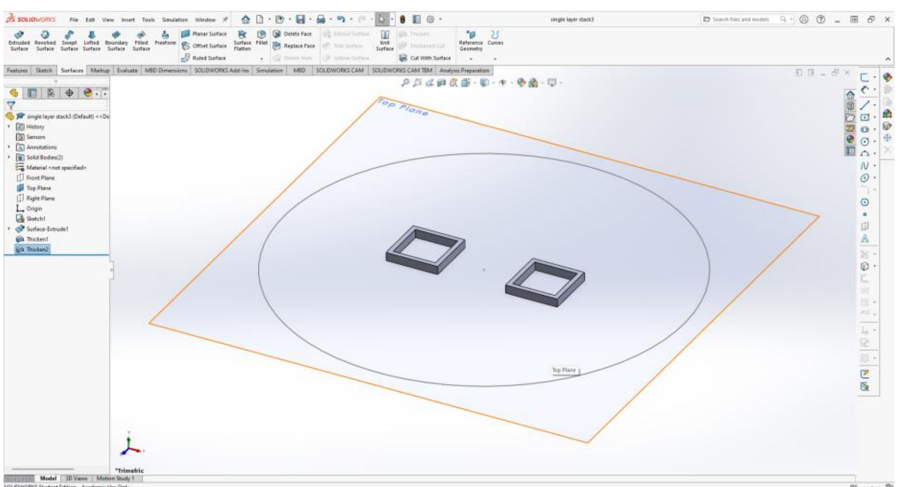

Figure 24: CAD Model of Two-Pass Stacked Geometry Used in All Stacking Trials

Each two-pass print was visually inspected for a range of characteristics relevant to stacking performance: edge definition, second-layer bonding, base-layer deformation, and the overall preservation of geometric intent. The prints were documented with photographs taken immediately after printing to capture both subtle differences and major failures before any deformation could occur due to continued curing or ambient movement.

The 15% THI-VEX material yielded the cleanest base layer appearance, but it struggled to maintain structural integrity during the second pass. After stacking, the second layer often appeared to slightly flatten the first, suggesting the material was too fluid to hold its shape against added pressure. This was especially evident at the edges, where the second pass caused the base layer to spread outward, visibly widening the print and softening the corners. In some cases, the upper layer merged into the base layer to such an extent that layer distinction was somewhat lost. Despite these shortcomings, the material extruded evenly and showed no signs of under-extrusion or flow starvation, which made it at least viable for applications that don't demand tight vertical resolution.

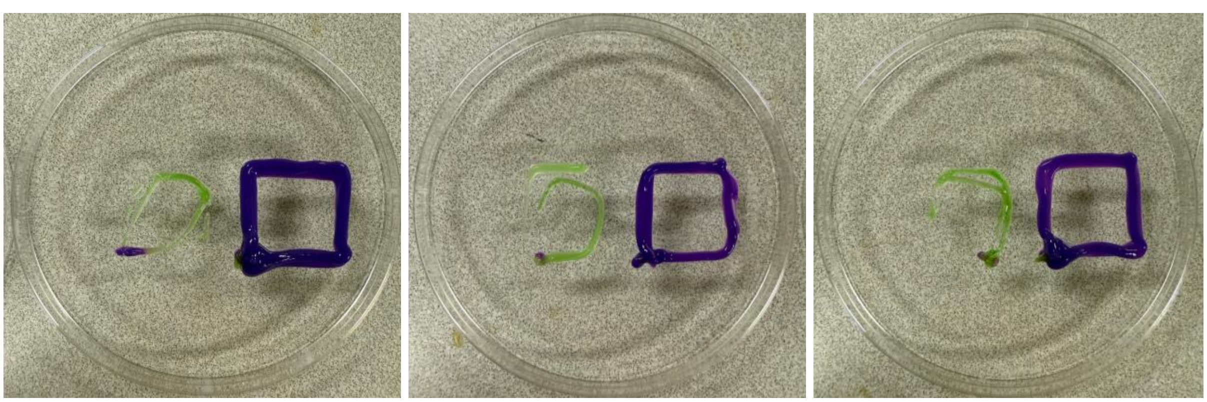

Figure 25: 15% THI-VEX Trial 1–3: Alternating Material Error

The 20% THI-VEX formulation performed significantly better in terms of layer separation and overall definition. Stacked prints maintained a clear distinction between the first and second pass, with little to no visible spreading at the edges. Corners remained sharp, and the upper layer retained its height without appearing to collapse into the base. This suggested that the material had enough stiffness to support vertical deposition while still bonding sufficiently with the layer below. While minor surface tapering was observed in some cases, particularly at the start and end points of each layer, the overall form held together consistently. Of the three materials tested, this formulation visually demonstrated the best balance between printability and structural fidelity.

The 25% THI-VEX prints offered little to no positive results. The increased viscosity did not help prevent spreading, and the resulting prints looked the messiest in terms of separation and definition. On top of that, the extrusion process was more variable: flow was less smooth, occasional air bubbles interrupted the material path, and one or both channels sometimes failed to deposit evenly. This led to prints where the second layer appeared incomplete or slumped unevenly over the base. In terms of visual structure alone, the 25% formulation showed no promise, and the increased mechanical resistance during extrusion introduced inconsistencies that reduced its reliability across trials.

Another subtle but important visual cue came from the edge taper at the perimeter of each square or line. For 25% THI-VEX, the edges tended to slope downward, suggesting spreading under the weight of the second layer. At 15%, the edges were much closer to vertical, and at 20%, they sometimes formed visible ledges, where the second layer sat rigidly atop the first. These observations added to the growing evidence that material stiffness—controlled through THI-VEX concentration—directly shaped the success of vertical deposition, but not without an upper limit as well as trade-offs in flow consistency and extrusion behavior.

These visual outcomes laid the groundwork for a more quantitative interpretation. In the next section, line and square widths will be analyzed to determine how much spreading occurred during stacking, and whether visual impressions matched measured structural behavior.

Repeatability and Qualitative Observations

In addition to documenting visual outcomes, each THI-VEX formulation was tested across three repeat trials to assess the repeatability of stacking behavior. All trials used the same geometry, print settings, and material prep procedures, with the only variable being the THI-VEX concentration. While perfect consistency wasn't expected, especially given the manual nature of syringe loading and nozzle swapping—the intent was to observe whether each formulation delivered predictable behavior under controlled conditions.

For the 15% THI-VEX group, repeatability was relatively high in terms of extrusion consistency. All three trials resulted in two-pass prints that looked nearly identical from a distance: smooth surfaces, fully extruded lines, and no print stoppages. However, the unwanted spreading of the base layer under the second pass was also consistent, which ultimately limited the structural value of these results. In every trial, the second layer caused the first to deform slightly outward, softening the edges and flattening the shape profile. While the prints were easy to produce, they repeatedly exhibited the same structural flaw: poor vertical definition.

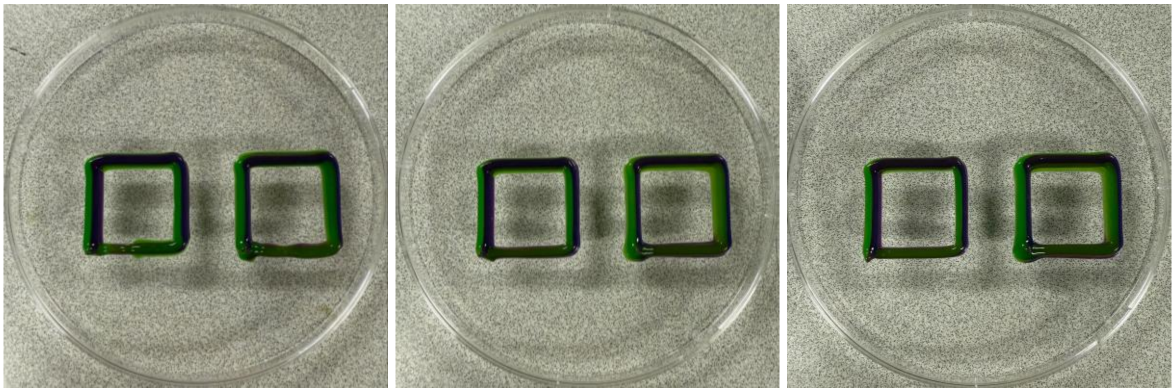

Figure 26: Trial Results - 15% THI-VEX

In the 20% THI-VEX group, results were not only visually better but also more reliable across all trials. In all three tests, the prints maintained clean boundaries between layers, with minimal edge tapering and a strong preservation of geometric intent. No extrusion failures were observed, and both print channels deposited material at a consistent rate. Although some minor variation occurred in how sharply the second layer terminated, especially at corners or line ends—these differences were subtle and did not compromise the overall structure. This consistency made 20% THI-VEX the most promising material from both a visual and process standpoint.

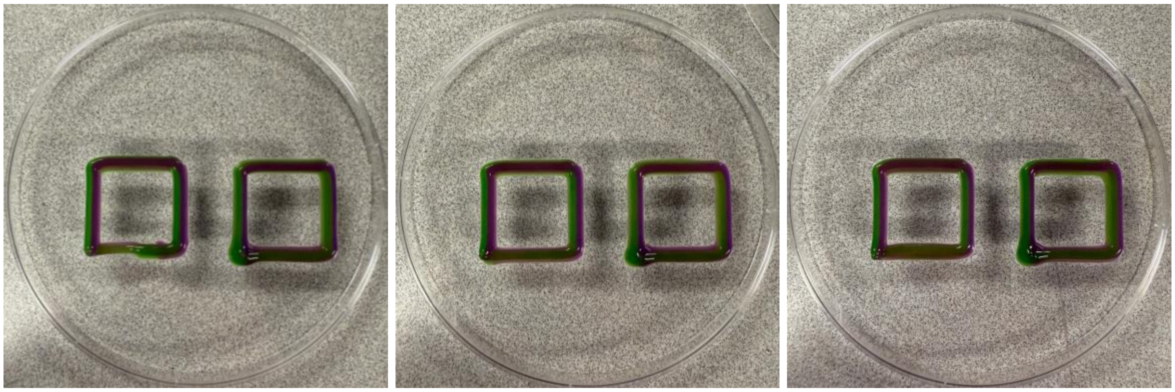

Figure 27: Trial Results - 20% THI-VEX

The 25% THI-VEX group demonstrated the most variability between trials. The formulation showed poor shape retention, the thicker mixture introduced flow inconsistencies that affected print reliability. In one trial, the second material channel failed to extrude completely, resulting in a one-sided stack with a skewed appearance. In another, air bubbles trapped during syringe loading emerged during deposition, leaving gaps in the upper layer. Only one of the three prints exhibited a clean, continuous stack with strong layer definition. This inconsistency suggested that while 25% THI-VEX was hoped to offer the best shape fidelity, it did not seem to settle under the same conditions as the other two groups. 25% carried too much risk of failure to be considered a dependable solution—at least with the current 15-minute pre-print curing window, syringe-based setup and nozzle configuration.

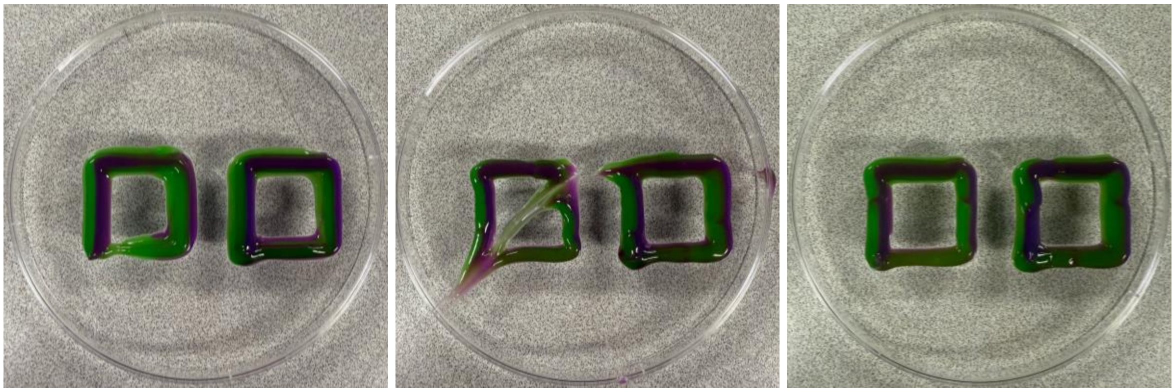

Figure 28: Trial Results - 25% THI-VEX

These qualitative results highlighted an important distinction: repeatability does not just depend on the material's stiffness, but also on how that stiffness interacts with extrusion mechanics. A more viscous material might theoretically perform better for stacking, but if it cannot flow reliably through the nozzle or maintain channel balance, the gains in shape retention are canceled out by practical modes of failure. In contrast, a slightly softer material that performs predictably and evenly may offer a better foundation for controlled Z-axis development, even if it doesn't produce the sharpest layer definition.

Overall, the 20% formulation struck the best balance between stiffness and flow, yielding visually strong and mechanically repeatable results across all trials. The consistency of its performance suggested it was the most viable candidate for further refinement or expansion into more advanced stacking experiments. It managed to avoid the common failure modes observed at the extremes—higher spreading in the 15% group, and flow breakdown in the 25% group—while maintaining layer separation and preserving shape.

This repeatability, combined with the visual observations in the previous section, provided a solid platform for transitioning into quantitative measurements. In the following section, line widths and square spacing will be analyzed to assess spreading behavior across materials and provide further insight into layer interaction quality.

4.3: Measurement & Print Quality Analysis

Line Width as a Proxy for Spreading

To move beyond visual inspection and validate earlier observations, each two-pass stacked print was measured to evaluate dimensional stability and material performance. The most telling metric in these trials was line width, used here as a proxy for spreading behavior. The logic is straightforward: in an ideal two-pass print, the second layer should deposit cleanly on top of the first, stacking vertically without deforming or displacing the base layer. If a print exhibited a significantly larger-than-expected width, it likely meant the second pass had flattened or displaced the base layer laterally, reducing stacking viability.

Calipers were used to measure the total width of each stacked line or square at three points—bottom, center, and top—on both the left and right prints in each trial. These values were then averaged to minimize error from small surface irregularities, nozzle wobble, or tapering at the ends. This approach ensured that the width values captured actual spreading effects, not just minor edge artifacts. All measurements were taken immediately after printing to eliminate the potential for post-cure deformation or surface settling to skew results.

Table 4: Caliper Measurements (mm) of Stacked Line Filament Diameter and Shape Spacing at Various Percentages of THI-VEX

THIVEX	Print Conditions	Square 1 Diameter: bottom	Square 1 Diameter: right	Square 1 Diameter: top	Square 2 Diameter: bottom	Square 2 Diameter: right	Square 2 Diameter: top	Distance Between 2 Squares
15%	5psi, 200mm/min	5.30	4.55	4.71	4.47	4.51	4.86	8.34
15%	5psi, 200mm/min	3.94	5.00	4.86	4.52	4.92	5.02	7.89
15%	5psi, 200mm/min	3.88	4.15	4.33	4.49	4.27	4.76	8.62
20%	5psi, 200mm/min	4.15	4.31	4.61	4.21	4.01	4.41	8.90
20%	5psi, 200mm/min	4.39	4.26	4.28	4.33	4.07	4.39	9.03
20%	5psi, 200mm/min	4.45	4.29	4.47	4.31	4.28	4.45	8.81
25%	5psi, 200mm/min	7.52	8.33	7.52	6.11	6.64	7.63	6.17
25%	5psi, 200mm/min	5.54*	5.63*	5.48*	5.24	7.44	7.38	N/A
25%	5psi, 200mm/min	5.29	6.52	7.58	5.91	7.75	7.62	7.26

*Measurement taken from lines with uneven distribution

Across all three material groups, distinct trends emerged. The 25% THI-VEX formulation resulted in the widest lines, with an average width of 6.73 mm, more than four times the internal nozzle diameter (1.59 mm). This clearly indicated that despite the formulation's visual sharpness, it did not translate to dimensional precision. The excessive spreading likely stemmed from poor interlayer bonding; instead of adhering cleanly, the second pass may have compressed the uncured base, pushing it outward rather than stacking it upward. Additionally, the stiffer formulation may have created internal resistance, preventing the top layer from bonding fully and instead deforming the structure. The widespread undermined any apparent advantage in layer separation.

In contrast, the 15% THI-VEX prints exhibited a moderate average width of 4.59 mm, suggesting good improvement in form retention compared to 25%, but still showing evidence of outward flow. This spread was likely caused by insufficient stiffness to support the weight of the second layer. The top pass visibly flattened the base, which remained soft and semi-liquid during deposition. Although extrusion was consistent across trials and no under-extrusion occurred, the softness of the material compromised stacking viability. The second layer often blended a bit into the first, creating a continuous mass rather than a distinct structure.

The most encouraging result came from the 20% THI-VEX formulation, which produced the narrowest average line width at 4.32 mm. While still wider than the nozzle diameter, this result indicated the second layer was able to sit atop the base without significant deformation or displacement. The balance of stiffness and extrudability in the 20% formulation was visibly apparent during printing and confirmed by these measurements. Unlike the 25% batch, which resisted extrusion and frequently failed during trials, the 20% mixture flowed evenly, adhered cleanly, and retained shape without spreading far beyond the intended geometry.

This outcome confirmed that increasing viscosity up to a point improves stacking performance by limiting material flow. However, it also demonstrated the limitations of assuming that more stiffness always equates to better stacking. The 25% formulation broke this trend, where added THI-VEX did not result in thinner lines, but instead caused worse deformation due to the material's inability to extrude or settle consistently. The data strongly suggest that 20% THI-VEX marks a functional upper limit—the sweet spot before stiffness becomes a hindrance rather than a help.

These findings align with theoretical expectations to a degree but also reveal the nonlinear relationship between viscosity and extrusion behavior in soft DIW printing. I initially hypothesized that increased THI-VEX concentration would yield progressively narrower prints, predicting the break point to occur somewhere above 25%. However, the data showed otherwise. The tipping point came sooner than expected, and the 25% prints not only failed to deliver tighter widths but actually exhibited the worst spreading overall. The real-world performance of these formulations proved more sensitive than anticipated, illustrating how thin the margin for successful stacking really is in silicone-based DIW.

Spacing Between Stacked Pairs

To complement the width analysis and gain a fuller understanding of print geometry, I also measured the spacing between adjacent stacked prints in each trial. Since each G-code trial deposited two identical structures side-by-side, this spacing served as a second useful metric: if both shapes retained their intended form, the distance between their outermost edges should remain close to the designed 10 mm gap. Any reduction in this spacing would imply that one or both shapes spread outward, encroaching on each other's footprint and potentially indicating structural compromise.

Using calipers, I measured from the outer left edge of the first square to the outer right edge of the second, averaging three values per trial to reduce error. These readings gave insight not just into individual print behavior, but also how consistently adjacent prints could maintain their positions—a key factor in multi-pass or multi-object printing.

As with the width measurements, the spacing data revealed some important differences between the three formulations. The 25% THI-VEX condition had the tightest average spacing at 6.715 mm, falling short of the intended 10 mm by 3.29 mm, or roughly 32.85%. This is a substantial deviation, and it backs up earlier observations that the stiffest formulation produced not only irregular flow but also significant deformation between prints. Despite appearing visually distinct in some trials, these prints physically collapsed into one another, clearly encroaching on the gap between them. Rather than preserving structure, the excess stiffness seemed to undermine it by resisting clean extrusion and disrupting layer formation.

The 15% THI-VEX formulation showed a solid improvement with an average spacing of 8.28 mm, amounting to an absolute error of 1.72 mm, or 17.2% off the target. While this was better than the 25% trials, it still indicated mild but consistent material spreading. The softer material tended to sag under the second layer's weight, slightly widening both shapes and shrinking the gap. In some cases, corners blurred and edges merged into slight tapers, all of which affected spacing.

Unsurprisingly, 20% THI-VEX once again performed the strongest, with a spacing average of 9.00 mm—only 1.00 mm short of the target, or 10% error. This small deviation indicates that the material retained its geometry with a high degree of precision. Unlike 15%, it didn't collapse under the second pass, and unlike 25%, it didn't resist flow in ways that caused distortion. The prints held their positions, preserved their shape, and didn't interfere with each other spatially—exactly the kind of behavior needed for multi-object layouts or denser stacking experiments.

These results further validate the idea that 20% THI-VEX sits in a practical sweet spot. It's stiff enough to prevent collapse but soft enough to flow consistently. The spacing metrics don't just support earlier observations—they also quantify them. And perhaps more importantly, they point out that increased viscosity doesn't guarantee dimensional precision. In fact, the 25% results show the opposite: a stiff material that performed the worst, both in measured spacing and in overall structural predictability.

While all three materials underperformed relative to the 10 mm spacing goal, only 20% did so within a tolerable margin. The other two fell short not just geometrically but functionally—they introduced enough variability that any future stacking tests using those concentrations would start on shaky ground. These spacing errors make it clear: when it comes to DIW stacking, material control isn't just about extrusion—it's about everything that happens after deposition too.

Identifying the Most Stable Material

With visual observations, dimensional measurements, and trial-to-trial repeatability considered, the selection of a stacking material becomes clear. 20% THI-VEX outperforms both alternatives by offering the most balanced performance across key metrics: flow consistency, layer definition, shape preservation, and inter-print fidelity.

The 15% THI-VEX formulation was the easiest to work with and showed good extrusion reliability. However, its softness and fluidity prevented it from maintaining shape under the pressure of a second layer. Spreading was visually apparent and confirmed by both line width and spacing data. While the prints were clean in isolation, they failed to meet the structural demands of Z-axis development. This makes 15% useful for demonstrations or single-layer prints but unsuited for stacking applications.

25% THI-VEX, on the other hand, promised higher precision due to its stiffness but failed in execution, with spacing values furthest from the intended geometry. The formulation frequently clogged nozzles, exhibited air bubbles, or failed to extrude evenly. Stiffness here became a liability—it undermined print consistency, created unpredictable flow paths, and led to premature failure. These limitations are especially problematic when scaling to multilayer tests, where even one failed layer can invalidate a print.

Only the 20% formulation avoided these pitfalls. It produced the narrowest usable lines, retained the intended spacing between stacked shapes, and demonstrated repeatable results across trials. It was stiff enough to hold form but still soft enough to extrude cleanly. It didn't clog or sag, and flattened the least under pressure. This balance—between structural integrity and process reliability—is exactly what's needed when pushing DIW into vertical geometries.

The results also reframe assumptions about viscosity. I initially expected stacking precision to increase continuously with more THI-VEX, believing a break point would occur somewhere beyond 25%. In practice, the break point came earlier than expected. Rather than improving precision, the 25% formulation introduced new failure modes that disrupted consistency. This non-linear behavior highlights the complex interactions between material properties, nozzle dynamics, and extrusion pressure in soft-material additive manufacturing. There's no single lever that guarantees performance—just a careful tradeoff between too little and too much.

As a result, 20% THI-VEX now serves as the baseline for future stacking trials. It offers the best compromise between shape control, extrusion success, and interlayer compatibility—three pillars necessary for any advancement beyond two-pass printing. The next steps, whether moving toward three-layer structures, alternating material compositions, or in-situ curing strategies, will depend on this formulation holding firm. And for now, it has.

4.4: Current Limitations and Next Steps Toward Multilayer Printing

Although the original goal of this phase included exploratory attempts at true multilayer stacking, testing concluded at the two-pass level. That decision wasn't due to mechanical failure or lack of interest, but instead stemmed from a combination of time constraints and a recognition that the material behavior, while improved, hadn't yet demonstrated the kind of control necessary to justify further complexity.

The most immediate factor was timing. With a full draft deadline approaching and two-pass data already collected and measured, it made more sense to shift into analysis than to pursue additional layers that would require another round of calibration, test setup, and print validation. Developing even a basic multilayer sequence would have meant new g-code, inter-pass delay logic, and a full system check to ensure the setup could handle Z-height increases without introducing new errors. The return on that investment at this stage felt uncertain—less like a continuation of the current work and more like a speculative side path.

The second reason was tied to performance. While the 20% THI-VEX formulation showed real improvement over the others, its results still didn't meet the threshold I'd consider technically viable for more advanced stacking. Line width measurements remained over 4.3 mm—more than 2.5x the nozzle diameter—and spacing between prints, though improved, still showed signs of lateral deformation. The best trials still didn't reach the level of specificity I was aiming for: ideally, extruded widths would fall within 0.5 mm of the nozzle size to signal meaningful control over vertical deposition. I hadn't expected that kind of precision to emerge in this round of testing, but with results falling short of that mark, it made less sense to build upward without first achieving that baseline.

That's not to say the material underperformed. The 20% THI-VEX blend consistently outpaced the others in terms of flow control, stacking integrity, and visual fidelity. But at this stage, the gains felt incremental rather than transformational. Additional testing would have been novel—certainly interesting—but not necessarily more informative, and I felt the data already collected offered a clear stopping point. Rather than stretch the process in pursuit of unproven returns, I chose to consolidate findings and define the test boundary.

That said, the two-pass trials do provide a solid platform for future multilayer work. If refinements like layer-specific curing windows, nozzle lift sequencing, or automated g-code pauses were integrated, the system would likely be ready for deeper exploration of Z-axis builds. And when that happens, the current results—especially those from the 20% formulation—offer strong starting parameters for extrusion timing, material choice, and geometry scaling.

Ultimately, the decision to pause here wasn't a failure to continue—it was a conscious effort to respect the limits of the current setup, define what had been learned, and leave the door open for the next step under better conditions.

Chapter 5: Future Work & Conclusion

5.1: Conclusions

This work replicated and extended a dual-material DIW process, originally developed by a previous student, to evaluate stacking capabilities in soft silicone systems. After validating the baseline system and materials, a nine-line matrix was designed to systematically explore extrusion performance across combinations of print speed and pressure. Results clearly indicated that only the 5 psi condition produced viable prints, with 200 mm/min identified as the optimal speed for consistent line formation.

With these parameters fixed, the focus shifted to vertical stacking through a two-pass test using three concentrations of THI-VEX: 15%, 20%, and 25%. Visual and dimensional measurements revealed that the 20% formulation delivered the best results—retaining structural shape, minimizing spreading, and maintaining consistent spacing between stacked features.

While multilayer trials were initially considered, the project concluded at the two-pass level. Still, the results demonstrate that targeted g-code refinements, combined with material tuning, can significantly improve stacking performance in soft-material DIW systems.

5.2: Limitations & Areas for Improvement

Testing was intentionally limited to two-pass stacking due to both timeline constraints and the dimensional performance ceiling observed in the results. Although the 20% THI-VEX condition showed the most promise, line widths remained over 4.3

mm—far from the 1.59 mm nozzle diameter, and well outside the 0.5 mm target range set for vertical precision.

In addition, the current system lacked support for layer-specific pause commands, in-situ curing, or adaptive Z-offset control. These features would be necessary to enable consistent bonding in multi-layer structures. Material preparation also introduced variability, particularly at higher THI-VEX concentrations, where extrusion became unreliable, and repeatability was difficult to achieve.

5.3: Future Work & Next Steps

Future work should focus on enabling true multilayer printing by integrating pause-and-cure functionality, adjustable Z-height between passes, and improved process automation. These additions would allow layers to partially cure before subsequent passes, minimizing spreading and increasing inter-layer adhesion.

Building on the findings of this study, the 20% THI-VEX formulation offers a stable baseline for more advanced stacking trials. With improved system control, tests could be expanded to explore greater global height, alternative geometries, and multi-material transitions. Rotational control of the nozzle could support angled or curved print paths, while streamlined material mixing protocols may reduce inconsistencies in extrusion.

These improvements would support more complex structures and bring the system closer to applications that demand both form fidelity and vertical build capacity.

References

[1] Paul, S., & Anand, B. (2015). A review on subtractive and additive manufacturing of metallic components. Procedia Manufacturing, 1, 37-45.

[2] Gibson, I., Rosen, D. W., & Stucker, B. (2015). Additive manufacturing technologies: 3D printing, rapid prototyping, and direct digital manufacturing. Springer.

[3] Hull, C. W. (1986). Apparatus for production of three-dimensional objects by stereolithography. U.S. Patent No. 4,575,330.

[4] Abdulhameed, O., Al-Ahmari, A., Ameen, W., & Mian, S. H. (2019). Additive manufacturing: Challenges, trends, and applications. Advances in Mechanical Engineering, 11(2), 1687814018822880. https://doi.org/10.1177/1687814018822880

[5] Zhou, L. Y., Fu, J., & He, Y. (2020). A review of 3D printing technologies for soft polymer materials. Advanced Functional Materials, 30(36), 2000187. https://doi.org/10.1002/adfm.202000187

[6] Stang, M., Tashman, J., Shiwarski, D., Yang, H., Yao, L., & Feinberg, A. (2023). *Embedded 3D printing of thermally-cured thermoset elastomers and the interdependence of rheology and machine pathing*. Advanced Materials Technologies, 8(6), 2200984. https://doi.org/10.1002/admt.202200984

[7] Smooth-On. (n.d.). EcoFlex 00-30 technical data sheet. Retrieved from https://www.smooth-on.com/products/ecoflex-00-30/

[8] Kim, J., Kwon, D., Seo, J., Shim, H. J., Jeong, H., Lee, J., & Kim, J. H. (2018). Soft electronics: Materials, manufacturing, and applications. Advanced Materials, 30(50), 1706913. https://doi.org/10.1002/adma.201706913

[9] Kechagias, J. (2022). Hybrid additive and subtractive manufacturing: Evolution of the concept. Materials, 15(5), 1724. https://doi.org/10.3390/ma15051724

[10] Duty, C., Ajinjeru, C., Kishore, V., Compton, B., Hmeidat, N., Chen, X., Liu, P., Hassen, A. A., Lindahl, J., & Kunc, V. (2018). *What makes a material printable? A viscoelastic model for extrusion-based 3D printing of polymers*. Journal of Manufacturing Processes, 35, 526-537. https://doi.org/10.1016/j.jmapro.2018.08.008

[11] Lawrence, C. (2024). Direct ink writing of silicone rubber for sensor applications [Master's thesis, University of Oklahoma].

[12] Abdollahi, S., Davis, A., Miller, J. H., & Feinberg, A. W. (2018). Expert-guided optimization for 3D printing of soft and liquid materials. PLOS ONE, 13(4), e0194890. https://doi.org/10.1371/journal.pone.0194890